Article ID: 1006-8775(2013) 04-0357-10

ANALYSES OF A MICROPHYSICAL RESPONSE TO THE SEEDING IN TWO CASES OF ARTIFICIAL FOG DISSIPATION

JIN Hua (金 华)[1,2], HE Hui (何 晖)[1,2], ZHANG Qiang (张 蔷)[1,2], HUANG Meng-yu (黄梦宇)[1], MA Xin-cheng (马新成)[1,2], ZHANG Lei (张 磊)[1], JI Lei (嵇 磊)[1,2]

(1. Beijing Weather Modification Office, Beijing 100089 China; 2. Beijing Key Laboratory of Cloud, Precipitation and Water Resources, Beijing 100089 China)

Abstract: Two field experiments were performed in order to dissipate the fog at Wuqing District of Tianjin in November and December of 2009. Hygroscopic particles were seeded to dissipate fog droplets on 6-7 November, 2009. Liquid nitrogen (LN) was seeded into the natural supercooled fog in the experiments of 30 November–1 December, 2009. Significant response was found after seeding. Significant changes were observed in the microstructure of fog in the field experiments. The of fog droplet changed dramatically; it increased first and then decreased after seeding. Remarkable variation also was found in the Liquid Water Content (LWC) and in the size of fog droplet. The Droplet Size Distribution (DSD) of fog broadened during the seeding experiments. The DSD became narrow after the seeding ended. After seeding, the droplets were found to be at different stages of growth, resulting in a transform of DSD between unimodal distribution and bimodal distribution. The DSD was unimodal before seeding and then bimodal during the seeding experiment. Finally, the DSD became unimodally distributed once again.

Key words: artificial dissipation of fog; microphysical changes; response

CLC number: P484 **Document code:** A

1 INTRODUCTION

Fog is a common weather phenomenon in the surface layer and it has great influence on human activities. Numerous field studies with focus on artificial fog dissipation were performed to reduce or avoid the financial and human losses related to fog and low visibility. Artificial fog dispersal is to destroy the colloidal, steady state by affecting some aspect of the water cycle based on different characteristics of fog, with a view to achieve the goal of fog dissipation. According to the temperature, fog can be divided into two categories: supercooled fog and warm fog.

There are not sufficient natural ice nuclei in supercooled fog and the most effective method to dissipate it is to seed with ice-forming material. Vardiman et al. has described an operational fog-dissipation system installed at Farichild Air Force Base, Washington[1]. During the winter of 1969–70, liquid propane was dispensed into supercooled fog to support aircraft landings and take-offs. During 1994–1997, liquid nitrogen was used to dissipate supercooled fog in field experiments at Beijing Capital International Airport and Shahe Airport[2]. Liquid nitrogen was selected as a seeding agent in the field experiment to dissipate supercooled fog in Tianjin in 2009.

The use of thermodynamics and dynamics is an effective way to dissipate warm fog, and it was adopted in field experiments of dissipating warm fog at Chengdu Shuangliu International Airport[3]. Pyrotechnic hygroscopic flares were ignited in the field experiment to dissipate warm fog in Tianjin in November 2009. Over the years, there have been many studies focusing on the possibility of modifying warm fogs with hygroscopic materials. Although the use of hygroscopic powders for the dissipation of fog has often been suggested, and in some instances actually tried previously, Houghton was the first person who has made a complete examination of the problem on a scientific basis[4]. To examine the concept of modifying fog with hygroscopic material, Jiusto et al. conducted an analytic and experimental

Received 2012-07-26; **Revised** 2013-08-06; **Accepted** 2013-10-15
Foundation item: National Natural Science Foundation of China (41205100, 41175007); National Department Public Benefit Research Foundation of China (GYHY201306065, GYHY200806001-4); State Key Development Program for Basic Research of China (2011CB403401); Central Level, Scientific Research Institutes for Basic R & D Special Fund Business (IUMKY201313PP0403)
Biography: JIN Hua, senior engineer, primarily undertaking research on cloud and precipitation physics.
Corresponding author: JIN Hua, e-mail: jinhuawm@gmail.com

investigation in 1968[5]. Results show that it is possible to improve visibility in warm fog by seeding with micron-size salt particles (NaCl). Simulation results from a two-dimensional Eulerian model of warm fog dispersal showed that seeding over a wide area can result in practically useful visibility improvements. The quantity of material and the cost of the wide-area seeding technique depend upon fog intensity, fog type, and wind speed[6]. A study by Silverman and Kunkel[7] showed that to achieve the same visibility improvement the seeding rate is directly proportional to the fog liquid water content and inversely proportional to the fog drop size. Studies above showed that it is possible to dissipate warm fog with hygroscopic material by knowledge of the microstructure of warm fog.

One of the most significant microphysical parameters describing cloud and fog is the drop size distribution (DSD) and it can also be called droplet size spectra or droplet spectra. DSD is often characterized by a function $n(r)$, which is defined such that $n(r)$dr is the number of droplets per unit volume in the radius interval (r, r+dr). There are many studies about DSD of fog since the 1960s. Eldridge discussed the variation characteristics of a few fog DSD and fog water liquid content which were observed by an instrument called Particle Counter[8]. It was observed that DSD at different development stage or location of cloud and fog can be either unimodal or bimodal (even multimodal). Observation from the cloud over Mount Washington showed that DSD was bimodal in character[9]. Stewart found multimodal aerosol distributions in fog in England[10]. Arnulf et al.[11] presented four families of DSD representing different stage of fog and these four stages are "selective", "evolving fog", "stable fog (1st type)" and "stable fog (2nd type)". A project of Canada (FRAM, 2005–2007) provides a better understanding of fog-induced low visibility and improves the parameterization of fog microphysics. Bimodal DSD was found in the continuous microphysical observation of fog in this project[12]. Neiburger and Chien[13] computed DSD as a function of time after the initiation of the droplet growth process. Their study showed that DSD is unimodal until after about 47 minutes have elapsed. At that time, the DSD becomes bimodal. Eldridge[10] analyzed the transformation of DSD between the "evolving fog" and the "stable fog". After comparing DSD of the "evolving fog" with the cloud DSD computed by Neiburger, he suggested that the existence of multimodal DSD in developing fog and cloud appears to be a true characteristic of the distributions, and that it seems reasonable to postulate a life history of fogs and clouds in terms of varying time dependent DSDs.

There are also many studies of fog DSD in China. After analyzing the microphysical characteristics of the fog which was observed in Beijing, Wang[14] suggested that the DSD was the main variable to characterize the evolving of the fog and that broadening of DSD is the main characteristics of the fog development. A relationship between liquid water content (LWC) and visibility was presented by Yang[15] who had analyzed microstructure of the fog observed off the coast of Qingdao between 1980 and 1982. After studying dense fog over the Nanling Mountains area in 1998 and 2001, Tang et al.[16] demonstrated that mean fog DSD of Nanling Mountains area shows a simple continuous decrease in number concentration (NC) which can be represented by a power law and that physical processes like condensation, collection and deposition developed asymmetrically during the development of the fog; Deng et al.[17] found that the NC of fog over Nanling Mountains area is smaller than that of urban area and the predominant proportion of fog is small droplet. Liu et al.[18] and Bao et al.[19] have observed different dense fog event at Nanjing separately, and they also analyzed the formation mechanism and the microphysical characteristics e.g. DSD, NC and LWC of fog. After analyzing DSD of a sea fog event that occurred in the South China Sea, Qu et al.[20] found that fog microphysical structure is closely related to fog development, and fog droplets are much larger in the initial stage. They suggested that during the period of upward development and vertical mixing of fog, fog droplets have local features and begin evaporating. The DSD and droplet NC of sea fog from 16 to 19 March 2008 were investigated in the Science Base for Marine Meteorology at Bohe, Guangdong province. The microphysical structure and the LWC of sea fog were analyzed. According to observational data during the same period, the synoptic factors accounting for the low atmospheric visibility associated with this sea fog event were also analyzed[21]. Besides analyzing the evolution of LWC characteristics of the high-pressure pattern of sea fog, Li et al.[22] also discussed the relationship between LWC and the average diameter and NC of fog droplets, air temperature, wind speed and turbulent exchange. Both bimodal DSD and multimodal DSD were found in the observations of Guangdong and Nanjing mentioned above.

There are few studies involved in the evolution mechanism of DSD and those on cloud DSD mainly focused on cumulus cloud. The updraft in stratiform cloud is weaker than in the cumulus cloud and the updraft in fog is also small, which is similar to the stratiform cloud. A mechanism named "ripening process" was introduced for DSD broadening in stratiform clouds. Çelik and Marwitz[23] have done some simulation with a cloud model to evaluate this mechanism. The description of the mechanism is as follows. A cloud DSD contains droplets with different size caused by different salinity. Small droplets have higher equilibrium supersaturation (s*) than the one

for larger droplets. Large droplets need the ambient supersaturation (s) to grow, thereby decreasing the s below the s* for small droplets, thereby causing them to evaporate. Even if s > s* for some of the small droplets, some small droplets will not grow as fast as large ones. Thus, a narrow droplet size spectrum will broaden to cover both large and small sizes. However, due to evaporation of small droplets this process will eventually narrow the DSD. In limited time, the DSD will contain droplets with uniform salinity and size (unisize spectrum). Thus, this process is a broadening process during the early stage (a few hours or longer); thereafter, it tends to be a narrowing process[23]. There are few studies involving the evolving the mechanism of fog DSD and there are even much fewer studies focusing on continuous variation of fog microphysical structure after the field seeding experiment for fog dissipation. Continuous variation of DSD was observed with a new instrument from the beginning to the end of the warm fog dissipation field experiment in Tianjin in 2009 and microphysical response of fog to seeding was also analyzed in this study. Since the procedures of this experiment were similar to that of the simulation which has been done by Çelik[23], the variation of DSD in the field experiment was compared with the simulation to help understand the variation process in the warm fog DSD and to contribute to the warm fog dissipation field experiment that will be conducted later.

2 FIELD EXPERIMENTS OF FOG DISSIPATION IN TIANJIN

Techniques employed to measure DSD may be grouped into two major classifications: first, those techniques in which the measured droplets make physical contact in some manner with a collector; and second, methods which do not use a collector. In past studies of China, DSD was measured by an instrument named triplex droplet collector which employed a technique of contacting: fog droplets were captured by a coated slide and the size and number of droplets were observed with a microscope. Small-sized droplets cannot be sampled with a triplex droplet collector for the sake of resolution limitation and it was also not suitable for continuous observation because of its low sample frequency. To find detailed variation of fog microphysical structure after seeding, a newly fog particle spectrometer (FM-100) was used in the field experiments in Tianjin. FM-100 can continuously sample at a frequency of 1 Hz and instead of a collector it employs a set of optical instruments and signal processor. The number and size of droplets were computed with the data of voltages which were transformed from the forward scattering light signal. FM-100 has been employed in field observations abroad for years (e.g. FRAM) and it firstly appeared in fog field studies in Guangdong and Jiangshu provinces of China in 2006[12, 18-22].

In 2009, fog dissipation field experiments were conducted by Beijing Weather Modification Office and roads near the Meteorological Bureau of Wuqing district, Tianjin were chosen as the site of seeding (Fig. 1). Besides the observations of temperature, relative humidity and visibility, two in-situ instruments were also used for characterizing aerosol and fog DSD. The size distribution of seeding particles released by pyrotechnic hygroscopic flares was measured with a Passive Cavity Aerosol Spectrometer Probe (PCASP SPP-200, 0.1–3 μm) and DSD of fog was observed with a fog monitor (FM-100, 2–50 μm). Both instruments were manufactured by Droplet Measurement Technologies Inc., Boulder, Co., U.S.A.

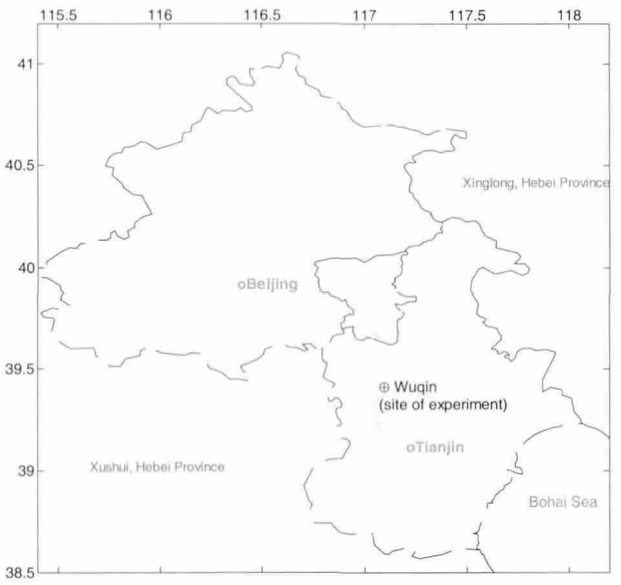

Figure 1. Location of field seeding experiments in 2009.

Mobile combustion equipment was installed on a trailer, which was towed by a vehicle to cycle along a section of road to dissipate warm fog on November 6. The PCASP was mounted on a car and was used to observe particles of the seeding agent released by burning flare. Different locations around the fixed observation field were chosen according to environmental factors (e.g., wind speed, wind direction) to disperse liquid nitrogen (LN) for the dissipation of supercooled fog on December 1, and total amount of the dispersed LN was 2.1 ton.

2.1 *Microphysical characteristics of warm fog on November 6-7 and the field experiment to dissipate warm fog*

2.1.1 NATURAL FORMATION AND DISSIPATION OF WARM FOG BEFORE AND AFTER THE FIELD EXPERIMENT

Fog appeared and developed slowly after the

midnight of November 5 at Wuqing District. Fog developed explosively following the decreasing of temperature before dawn of November 6 and the visibility decreased sharply from 200 m to 40 m between 03:42 (Beijing Standard Time, the same below) and 03:45. Fog dissipated naturally with increasing intensity of solar radiation and temperature. Visibility rose to about 800 m at noon and reached a maximum of 900 m before 15:00. Visibility decreased with decreasing temperature and it reduced to a minimum of 14 m at 19:00 with the regeneration of fog. Development of fog at November 6 indicated apparently diurnal variation, which is a typical characteristic of radiation fog (Fig. 2).

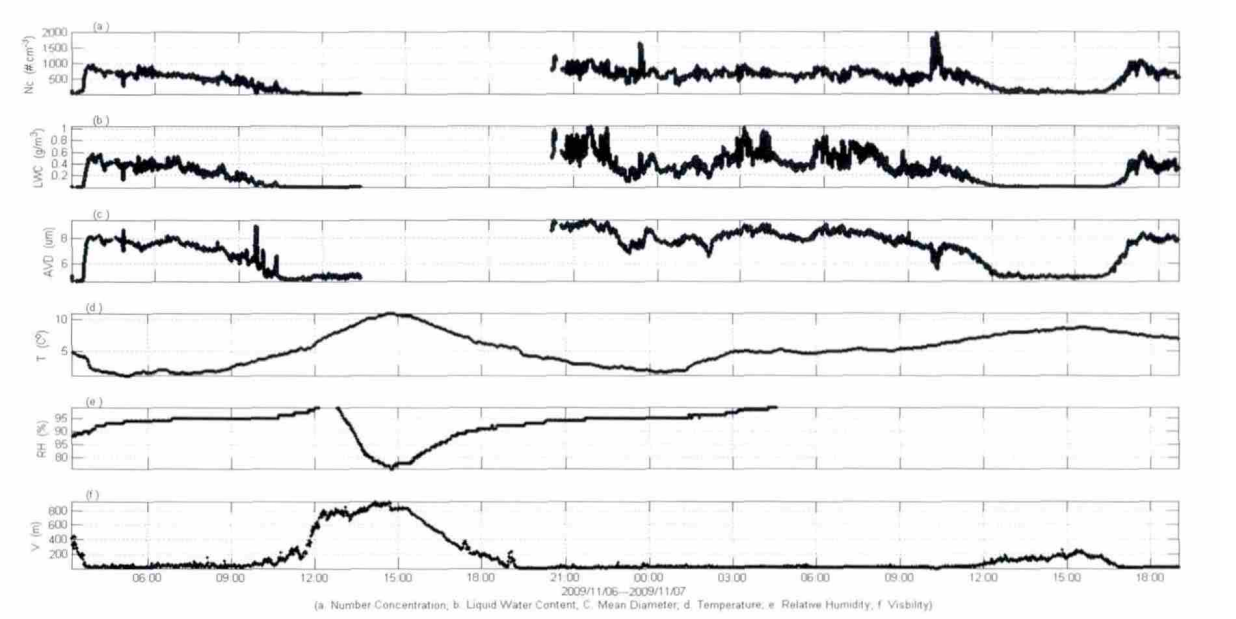

Figure 2. Microphysical characteristics of fog on November 6-7.

Mean NC of fog droplets was 477 cm^{-3} and mean LWC of fog droplets is 0.27 g m^{-3} during November 6. The NC of fog droplet rose from a few tens to 1000 cm^{-3} between 03:20 and 03:50, which is the formative stage of fog. During this stage, the LWC rose from 0.01 to 0.5g m^{-3} and the width of DSD broadened from less than 5 to 13 μm. At the beginning of the formative stage, the fog DSD showed a simple continuous decrease in NC and changed to be unimodal at the end of this stage. During the mature stage of fog, the NC of fog droplet varied from 500 to 1000 cm^{-3}, the LWC was 0.2–0.5 $g.m^{-3}$, fog DSD primarily remained to be unimodal and the width of DSD was broader than 10 μm. During the dissipative stage of fog, the NC of fog droplet decreased to less than 100 cm^{-3}, the LWC was less than 0.1 $g.m^{-3}$ and the width of DSD narrowed to be less than 5 μm. The fog DSD transferred to be a simple continuous decrease in NC again at the end of this stage. When the fog was in its most dense duration, the maximum of NC was 1000 cm^{-3} and the LWC exceeded 0.5 g m^{-3}.

Development of fog at November 7 showed also a diurnal variation in which visibility rose to 200 m between 12:00 and 15:00 and thereafter decreased again (Fig. 2). Mean NC was 516 cm^{-3} and mean LWC was 0.31 $g.m^{-3}$ during November 7 and they were the maximum mean values all over this fog event. Visibility rose to 1000 m after 07:00 November 8 and the whole fog event ended thereafter.

When the warm fog developed naturally at the beginning of the formative stage, the DSD showed a simple continuous decrease in NC. The DSD became unimodal and the width of DSD broadened at the mature stage of fog. And the DSD transferred to be a simple continuous decrease in NC again and the width of DSD narrowed at the dissipative stage of fog (Fig. 3).

2.1.2 FIELD EXPERIMENT TO DISSIPATE WARM FOG AND MICROPHYSICAL VARIATION OF WARM FOG

Seven flares were used during the first field experiment to dissipate warm fog which began at 22:00 November 6 and the experiment field was 1 km away from the Meteorological Bureau of Wuqing District. The maximum value of visibility, which was observed after seeding, was about 300 m while being about 40 m before seeding. The second field experiment to dissipate warm fog was conducted on roads around the Meteorological Bureau of Wuqing District between 23:35 November 6 and 00:05 November 7. The temperature was about 2℃ during the second experiment and 7 flares were used. Visibility varied from 20 to 90 m and the fog was observed with a fog monitor during this experiment.

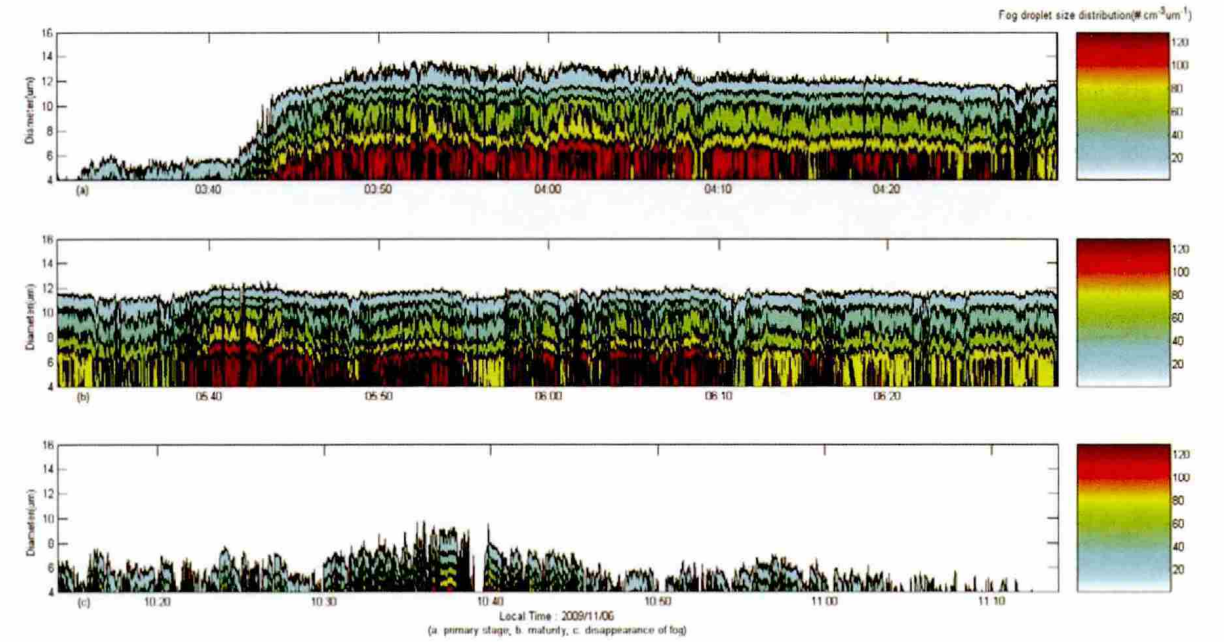

Figure 3. Droplet size distribution of fog at different evolution stage.

2.1.2.1 MICROPHYSICAL CHARACTERISTICS OF PARTICLES RELEASED BY PYROTECHNIC HYGROSCOPIC FLARES

According to the PCASP data, the NC of aerosol particles increased dramatically and reached its maximum soon after seeding while the effective diameter of the seeding particles was small. According to the particle size spectra of aerosol, diameter of the added particles was between 0.2 and 0.4 μm and the mode diameter was 0.3 μm while the width of DSD was 0.6 μm. It was determined that the added particles mainly consist of seeding agent because of the corresponding relation between the maximum NC and the seeding time.

2.1.2.2 MICROPHYSICAL VARIATION OF WARM FOG AFTER SEEDING

During the second field experiment to dissipate warm fog, NC and LWC rose to their maximum value while the diameter of fog droplets decreased between 23:35 and 23:39. Two minutes later, NC decreased while the diameter of fog droplets was increasing; big particles larger than 10 μm in diameter were found, the width of DSD broadened, the DSD changed from unimodal to bimodal and the diameter of the second peak was 9 μm. The next seeding was conducted between 23:41 and 23:44 November 6 and the variation mentioned above occurred again. After seeding, NC decreased while the diameter of fog droplets and LWC were increasing, the width of DSD narrowed and the DSD changed back to be bimodal (Fig. 4).

2.2 *The field experiment to dissipate supercooled fog on December 1*

2.2.1 BRIEF INTRODUCTION TO THE FOG EVENT AND THE EXPERIMENT

Visibility was getting worse between 20:00 and 23:00 on November 30. The maximum lapse rate of surface temperature is 1.7℃ h^{-1} between 00:30 and 01:30, which was the formative and developing stage of fog. Visibility was 500 m at the beginning of this duration and it reduced to 50 m in the end. Visibility remained to be less than 100 m between 01:00 and 09:00, which was the mature stage of the supercooled fog. Visibility rose and exceeded 700 m between 10:00 and 11:00, which was the dissipative stage of supercooled fog (Fig. 5). Characteristics of fog DSD in different stage on December 1 were similar to that of warm fog on November 6 except that temperature was below 0℃ in the whole fog event of December 1 and it was a supercooled fog event.

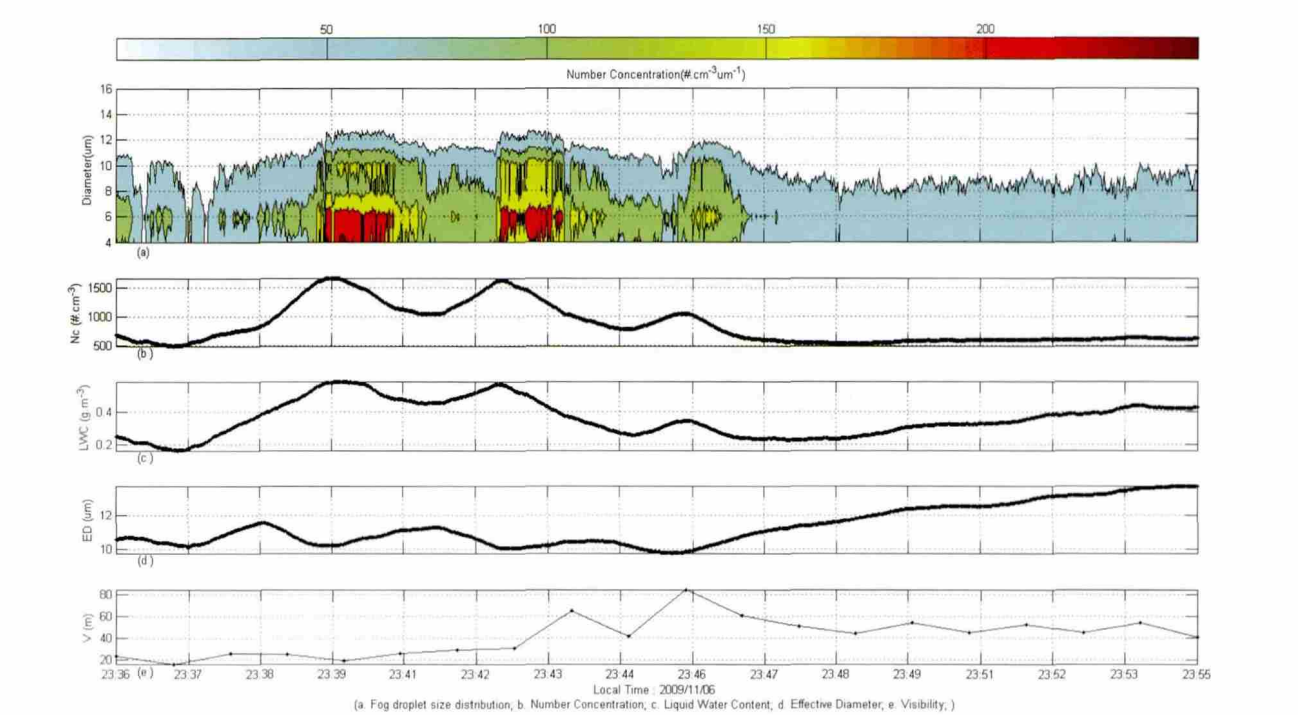

Figure 4. Evolution of fog microphysical characteristics during seeding on November 6-7. (a): fog DSD; (b): NC; (c): liquid water content; (d): effective diameter; (e): visibility.

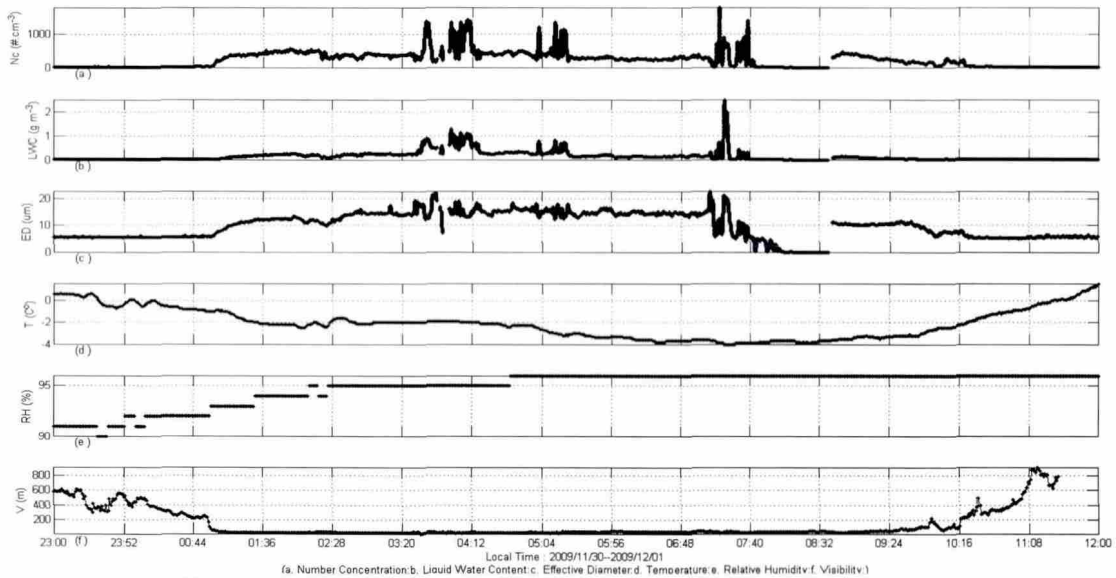

Figure 5. As in Fig. 2 except for fog between November 30 and December 1.

There was no significant variation of visibility during the field experiment to dissipate supercooled fog on December 1. The fog monitor was not set in the diffused zone of LN in the third seeding. Severe microphysical variations were observed in all the seeding operation except the third and the seeding operation between 05:00 and 05:15 was taken as an example for analysis.

2.2.2 MICROPHYSICAL VARIATION OF SUPERCOOLED FOG AFTER SEEDING

After seeding, NC first rose sharply to the maximum of 1800 cm^{-3} and dropped remarkably to the value of 400 cm^{-3} later. It was found that the fog DSD varied significantly and bimodal DSD was also found during seeding (Fig. 6). Several bimodal DSD repeated quickly and DSD gradually changed from the simple decrease type to the unimodal type and the bimodal type just after the first bimodal DSD appeared after seeding. DSD changed back to be unimodal from being bimodal after the impact of seeding was over.

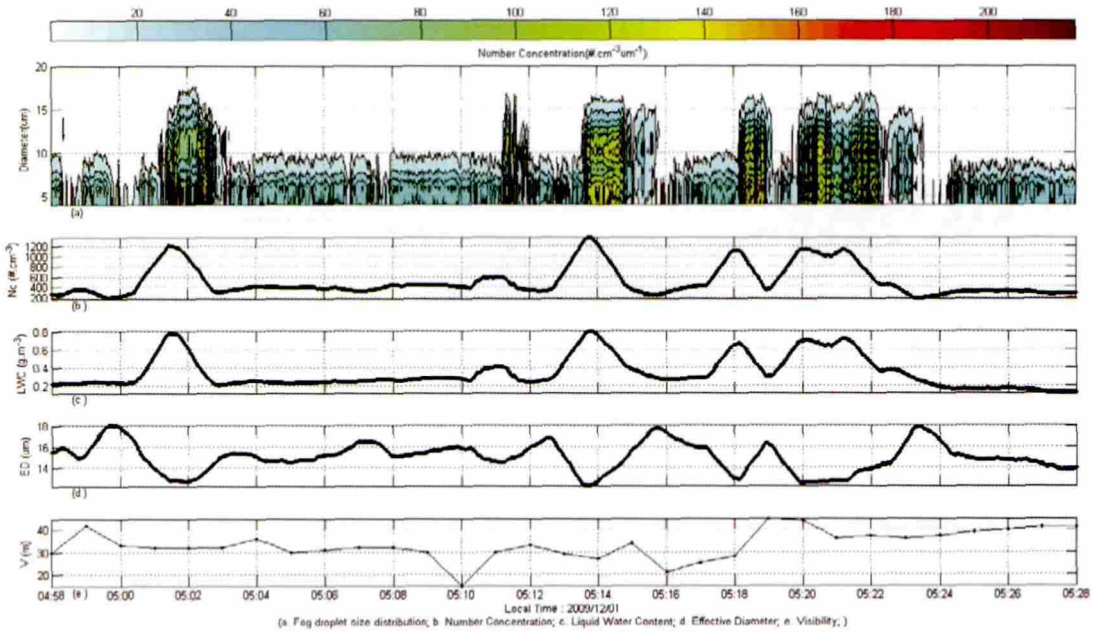

Figure 6. As in Fig. 4 except for fog on December 1.

3 DISCUSSION

3.1 *Analysis of the microphysical response to the seeding*

After seeding, double peak values of the bimodal DSD in warm fog were 4–6 μm and 9–10 μm respectively while the width of seeding agent particles spectra was 0.6 μm. It showed that the change of fog DSD was not the direct result of the dispersing of seeding agent particle but the result of the change in the microphysical structure of fog.

Figure 7 shows the composition and variation of different size fog particles in the field experiments of dissipating the fog. The fog particles were divided into two subsections according to the size of the diameter. Fog particles with a diameter larger than 6 μm were defined as large particles (Nr>6, red circle) while diameter of small fog particle was less than 6 μm (Nr<6, blue point). In order to facilitate the analysis of warm fog data in the seeding experiment, the large particles and small particles data were normalized with their maximum respectively. Relative evolution of the fog NC maximum was plotted in Fig. 7. The black line indicates the proportion of small fog particles. So the area below the black line represents the proportion of small fog particles and the area above the black line means the proportion of large particles. The variations of fog particles with different size after the seeding experiment are as follows. The increasing rate of large particles is higher than that of small particles and it is especially true in the field experiments of dissipating supercooled fog. The proportion of large particles rose significantly before dropping later and finally restored to the situation before the seeding experiment. During some specific time periods, the increase of the proportion of large particles and the decrease of the proportion of small particles occurred simultaneously.

The proportion of large particles significantly increased, which showed that the seeding effect did really occur. While the affected area of a particular quantity seeding agent was limited, as unaffected fog mass has spread to the observation site after the seeding agent spread to the surrounding area, the proportion of large particles decreased later.

To verify the role of the ripening process during the steady-state stage in a cloud, Çelik used a Lagrangian cloud model to perform different numerical simulations with different Cloud Condensation Nuclei (CCN) spectra. Conditions of numerical tests were as follows. The updraft of a cloud parcel was zero and the largest size of the CCN particles was assumed to be 0.5, 0.6, 0.7, 0.8, 0.9, 1.0, 1.1, and 1.2 μm. Ambient vapor is saturated while the supersaturation is small. Droplets with different hygroscopicity competed for the ambient vapor to grow up. The conditions for the field experiment to dissipate warm fog in Tianjin were similar to that of the simulations mentioned above. Results of simulations of Çelik were as follows. Bimodal DSD appeared when the ripening process was active after the saturation reached its peak. Another result of the ripening process was the decreasing of NC while the mean size of the droplet was increasing[23]. Bimodal DSD appeared while the width of the DSD was broadening first in the field experiment to dissipate warm fog. Then NC decreased while the mean size of the droplet was rising (23:39–23:41 in Fig. 4). It was also found that the proportion of large fog particles increased while the proportion of small fog particles was decreasing. These results were similar to that of

the simulations performed by Çelik. Similarity in conditions and results can be found between simulations performed by Çelik and the field experiment in question. It can be deduced that the ripening process has happened in the warm fog after seeding.

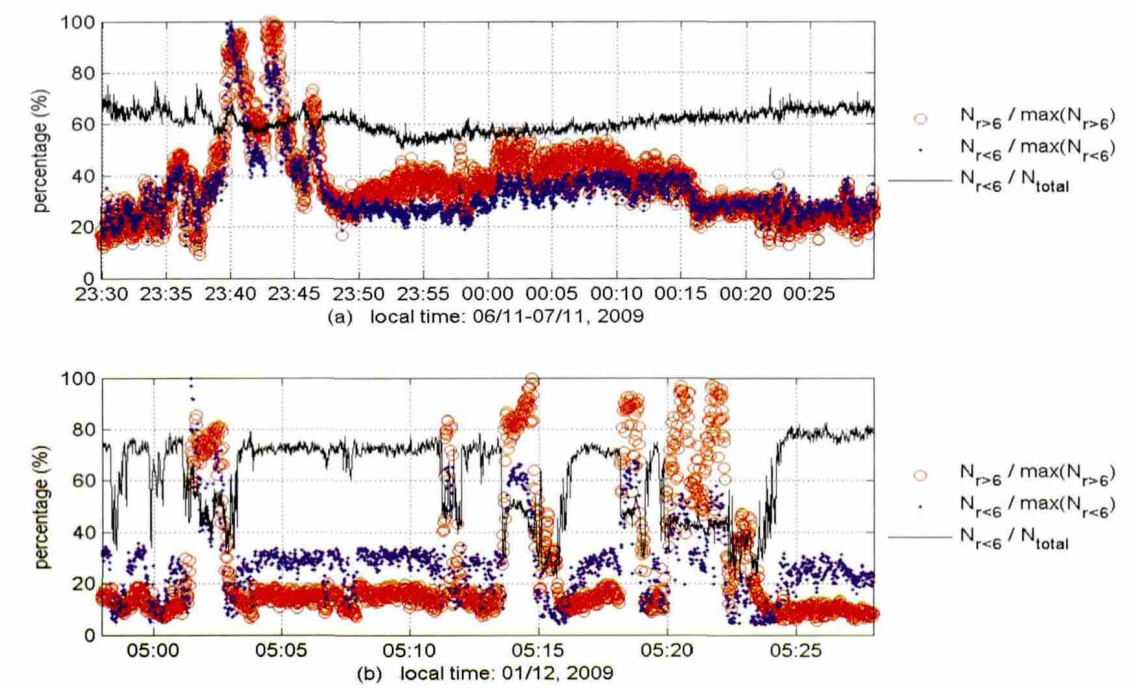

Figure 7. Composition and variation of different size particles in the fog during the seeding experiment. Particles with a diameter larger than 6 μm are indicated with a red circle (Nr>6, red circle) while the blue point indicated particles less than 6 μm (N<6, blue point). The black line indicated the proportion of small fog particles less than 6 μm.

Large number of supercooled fog droplets existed in the form of supercooled LWC and the Bergeron process would happen quickly if heterogeneous freezing nuclei were introduced. Plenty of small fog droplets evaporated and disappeared while a few bigger ice crystals were forming, so the proportion of large fog particles rose while the proportion of small fog particles was decreasing, just as in the case of 05:04 and 05:15 in Fig. 7b.

The DSD was unimodal when the warm fog and supercooled fog developed naturally during November and December in Tianjin. Large particles increased rapidly after seeding (Fig. 7) while the width of the DSD was broadening and the fog DSD was changing quickly from unimodal to bimodal (Fig. 4 and Fig. 6). The time period for bimodal DSD to form was significantly reduced as compared with the simulations performed by Neiburger et al.[13] and Çelik et al.[23]. It can be deduced that the fog had developed into another stage and the fog natural development process was changed and accelerated. These results were in accordance with the principle of fog dispersal, which manages to accelerate the natural development of fog and shorten the fog lifetime.

In summary, a new process (e.g. Ripening process of warm fog and Bergeron process of supercooled fog) has occurred in the fog after seeding. Plenty of large newborn particles and their increasing proportion in the fog have a direct causal relationship with the seeding operation. A series of phenomena, such as conversions between DSD of unimodal and bimodal distribution and broadening of the DSD width, were found in fog after seeding and they can be deduced to be the microphysical response to the seeding operation in the field experiments of dissipating the fog.

3.2 *Possible mechanisms of variation of fog DSD after seeding operation in warm fog*

Mechanisms of the bimodal DSD formation in warm fog and supercooled fog after seeding are different. The hygroscopicity of seeding agent particle is better than that of natural cloud condensation nuclei after seeding in a warm fog. Fog droplets with a nucleus of seeding agent particles grew up more quickly and became larger than the droplets with a natural nucleus, which resulted in broadening of DSD width. The newborn fog droplets competed for water vapor to grow up after the ripening process was activated, resulting in the evaporation and decreasing of natural small fog droplets. Mixture of different fog droplets caused by turbulence was the possible reason of the bimodal DSD which was observed after seeding in warm fog.

3.3 *Possible mechanism of variation of fog DSD after seeding operation in supercooled fog*

Evaporation of the dispersed LN lowered ambient temperature and some aerosol particles were activated to serve as ice nuclei, leading to the start of the Bergeron process. Liquid water transferred quickly from fog droplets to ice nuclei and the ice crystal grew up to be new large particles which composed one peak of the bimodal DSD. Another peak of the bimodal DSD was composed of natural fog droplets. Mixture of different fog particles caused by turbulence possibly accounts for the bimodal DSD which was observed after seeding in supercooled fog. The newborn ice crystal consumed large amount of liquid water to grow up after seeding. Sedimentation of the grown ice particle caused the fog particles NC to decrease sharply. It could possibly explain why the NC sharply increased first and decreased later.

3.4 *Relationship between the LWC and the development of warm fog droplets after seeding*

The second field experiment to dissipate warm fog was conducted between 23:35 November 6 and 00:05 November 7. Minimum of the LWC before seeding was observed at 23:34:04 November 6. Maximum and minimum of the LWC after seeding were found at 00:02:19 and 01:04:03 November 7 respectively. An acceptable fitting curve described by the following equation can be obtained with the datum at the three moments of time mentioned above (confidence interval at 95% and figure with the fitting curve not shown):

$$n(r) = ae^{br}+ce^{dr} \quad (1)$$

where $n(r)$ is the fog DSD function in (cm^{-3} μm^{-1}), and values of a, b, c and d are listed in Table 1.

Table 1. Microphysical parameters of fog during the second experiment on November 6-7.

Time	N(cm^{-3})	LWC(g m^{-3})	$r_m^{"}$ (μm)	a	b	c	d
23:34:04 Nov. 6	450.11	0.0898	3.2446	-1054.0	-0.1240	1240.0	-0.1327
00:02:19 Nov. 7	924.18	0.7645	5.4837	5647.0	0.3321	-6343.0	-0.3776
01:04:03 Nov. 7	228.10	0.0918	4.0304	545.2	-0.1642	-442.2	-0.1541

N_i is NC of a group which is defined as the number of droplets per unit volume in the radius interval (r_i+△r/2). Total number of fog droplets per unit volume (N) was the NC of fog droplets. Cube root radius is a variable to denote the mean volume or the mean mass of the droplets and it was introduced to discuss the relationship between size and NC in the case of LWC variation was fixed. $r_m^{"}$ is the cube root radius and the equation is as follows.

$$r_m^{"} = \left(\frac{\sum r_i^3 n_i}{N}\right)^{\frac{1}{3}} \quad (2)$$

N is the NC of fog droplets and its equation can be deduced to be $N = \frac{3LWC}{4\pi\rho_w r_m^{"3}}$ from the equation of $LWC = \frac{4}{3}\pi\rho_w N r_m^{"3}$.

N is directly proportional to LWC when $r_m^{"}$ was fixed and $N_b = N_a \frac{LWC_b}{LWC_a}$.

If the cube root radius was kept constant, the NC should be increased from 450.11 to 3,831.40 cm^{-3} to produce the same variation of LWC as the observation.

$r_m^{"3}$ is directly proportional to LWC if N was kept constant and $r_{mb}^{"} = r_{ma}^{"}\left(\frac{LWC_a}{LWC_b}\right)^{\frac{1}{3}}$. If the NC was kept constant, the cube root radius should be increased from 3.2446 to 6.6249 μm to produce the same variation of LWC as the observation.

4 CONCLUSIONS

(1) Significant variation of NC, LWC and the size of fog droplets was observed after seeding. NC increased firstly and then decreased, with a sharp variation.

(2) Fog DSD was found to become broad during seeding. After seeding, the width of fog DSD became similar to its value before seeding.

(3) One result of the seeding effect is the appearance of droplets in different development stage. Another result of the seeding effect is the conversion between DSD of unimodal and bimodal distribution. The fog DSD was unimodal before seeding and bimodal during seeding. The bimodal DSD appeared again and again for several times and they all kept for little time. The fog DSD changed gradually from continuous simple decrease DSD to unimodal DSD and bimodal DSD after the first bimodal DSD appeared. DSD changed back to be unimodal from bimodal after the seeding was over.

(4) It can be deduced from the microphysical variation of fog operation that new processes were occurring in the fog after seeding. It could be concluded that the ripening process may have occurred in warm fog and the Bergeron process may have occurred in supercooled fog after the seeding operation.

Acknowledgement: Thanks for the recommendations of Xuexi Tie (Scientist of NCAR) on this work.

REFERENCES:

[1] VARDIMAN L, FIGGINS E D, APPLEMAN H S. Operational dissipation of supercooled fog using liquid propane [J]. J. Appl. Meteor., 1971, 10(3): 515-525.
[2] CAO Xue-cheng, WANG Wei-min. Collected papers of artificial dissipation of supercooled fog by using liquid nitrogen [M]. Beijing: China Meteorological Press, 1999.
[3] LI Zi-hua. Studies of fog in China over the past 40 years [J]. Acta Meteor. Sinica, 2001, 59(5): 616-624 (in Chinese).
[4] HOUGHTON H G. The transmission of visible light through fog [J]. Phys. Rev., 1931, 38(1): 152.
[5] JIUSTO J E, PILIÉ R J, KOCMOND W C. Fog modification with giant hygroscopic nuclei [J]. J. Appl. Meteor., 1968, 7(5): 860-869.
[6] WEINSTEIN A I, SILVERMAN B A. A numerical analysis of some practical aspects of airborne urea seeding for warm fog dispersal at airports [J]. J. Appl. Meteor, 1973, 12(5): 771-780.
[7] KUNKEL B A, SILVERMAN B A. A comparison of the warm fog clearing capabilities of some hygroscopic materials [J]. J. Appl. Meteor. Climatol., 1970, 9(4): 634-638.
[8] ELDRIDGE R G. A few fog drop-size distributions [J]. J. Meteor., 1961, 18(5): 671-676.
[9] ELDRIDGE R G. Measurements of cloud drop-size distributions [J]. J. Meteor., 1957, 14(1): 55-59.
[10] ELDRIDGE R G. Haze and fog aerosol distributions [J]. J. Atmos. Sci., 1966, 23(5): 605-613.
[11] ARNULF A, BRICARD J, CURE E, et al. Transmission by haze and fog in the spectral region 0.35 to 10 microns [J]. JOSA, 1957, 47(6): 491-497.
[12] GULTEPE I, HANSEN B, COBER S G, et al. The fog remote sensing and modeling field project [J]. Bull. Amer. Meteor. Soc., 2009, 90(3): 341-359.
[13] NEIBURGER M, CHIEN C W. Computations of the growth of cloud drops by condensation using an electronic digital computer [J]. Geophys. Monogr. Ser., 1960, 5: 191-210.
[14] WANG Geng-chen. An analysis of the microphysical structure of fog [J]. Acta Meteor. Sinica, 1981, 39(4): 452-459 (in Chinese).
[15] YANG Lian-su. A preliminary observations of the microphysical structure of fog in Qingdao area [J]. Marine Sci., 1985, 9(4): 49-50 (in Chinese).
[16] TANG Hao-hua, FAN Shao-jia, WU Dui, et al. Research of the microphysical structure and evolution of dense fog over Nanling mountain area [J]. Acta Sci. Nat. Univ. Sunyatseni, 2002, 41(004): 92-96.
[17] DENG Xue-jiao, WU Dui, YE Yan-xiang. Physical characteristics of dense fog at Nanling mountain region [J]. J. Trop. Meteor., 2002, 18(03): 227–236 (in Chinese).
[18] LIU Duan-yang, PU Mei-juan, YANG Jun, et al. Microphysical structure and evolution of a four-day persistent fog event in Nanjing in December 2006 [J]. Acta Meteor. Sinica, 2010, 24(1): 104-115.
[19] BAO Lei, YANG Jun, WANG Wei-wei, et al. Microphyrsical characteristics of a winter fog event in Nanjing [J]. J. Anhui Agri. Sci., 2009, 37(028): 13700-13701 (in Chinese).
[20] QU Feng-qiu, LIU Shou-dong, YI Yan-ming, et al. The observation and analysis of a sea fog event in South China Sea [J]. J. Trop. Meteor., 2008, 24(5): 490-496 (in Chinese).
[21] HUANG Hui-jun, HUANG Jian, MAO Wei-kang, et al. Characteristics of liquid water content of sea fog in Maoming area and its relationship with atmospheric horizontal visibility [J]. Acta Oceanol. Sinica, 2010, 32(02): 40-53 (in Chinese).
[22] LI Xiao-na, HUANG Jian, SHEN Shuang-he, et al. Evolution characteristics of liquid water content for a high-pressure pattern of sea fog [J]. J. Trop. Meteor., 2010, 26(1): 79-85 (in Chinese).
[23] ÇELIK F, MARWITZ J D. Droplet spectra broadening byripening process. Part I: Roles of curvature and salinity of cloud droplets [J]. J. Atmos. Sci., 1999, 56(17): 3091-3105.

Citation: JIN Hua, HE Hui, ZHANG Qiang, et al. Analyses of a microphysical response to the seeding in two cases of artificial fog dissipation. *J. Trop. Meteor.*, 2013, 19(4): 357-366.